LIN Hao, HAN Bingying, LING Lixia, *et al*. Pd_1-M (M=Al, Cu) Single-atom Catalysts for CO Oxidative Coupling to DMO: a DFT Study[J]. Coal Conversion, 2019, 42(4): 80-88. DOI: 10.19726/j.cnki.ebcc.201904011.

Pd_1-M (M=Al, Cu) Single-atom Catalysts for CO Oxidative Coupling to DMO: a DFT Study*

LIN Hao[1] HAN Bingying[2] LING Lixia[1,3] LIU Ping[3]
ZHANG Riguang[2] WANG Baojun[2]

ABSTRACT In order to reduce the amount of noble Pd catalyst in CO oxidation coupling to dimethyl oxalate (DMO). Two kinds of single-atom catalysts (SACs) were designed by density functional theory (DFT). The influence of Pd_1-M (M=Al, Cu) single-atom catalysts on the reaction were studied in detail. Firstly, it is found that Pd_1-Al SAC has a great surface deformation, which cannot exist stably, therefore it is not suitable for this reaction as a catalyst. Secondly, Pd_1-Cu SAC has shown an outstanding activity for the synthesis of DMO, and it achieves the goal of reducing Pd consumption at the same time. But the selectivity of Pd_1-Cu SAC to DMO is unsatisfactory and needs to be further improved in the future studies.

KEYWORDS CO oxidative coupling to DMO, single-atom catalysts, Pd catalyst, density functional theory

CLC number TQ426

DOI: 10.19726/j.cnki.ebcc.201904011

开放科学(资源服务)标识码(OSID):

0 Introduction

Single-atom catalysts (SACs) are new catalysts, which can minimize the size of the metal clusters and evenly distribute the active centers to the limit[1-2]. Past studies have shown that SACs have different properties and characteristics compared to traditional catalysts, such as significant size effect[3] and the low coordination environment of active metal center[4]. With the continuous development of catalyst preparation technology, SACs have been successfully prepared in experiment[5]. Furthermore, SACs also exhibit excellent catalytic performance in a large number of chemical reactions[6-13]. Because of the unique properties of SACs, studying the catalytic mechanism of SACs has a great significance for understanding the nature of catalytic reactions.

CO oxidative coupling to dimethyl oxalate (DMO) is an important part of C_1 chemistry[14-15]. In addition, the reaction is also the key technology to relieve the problem of the energy crisis in our country[16-17]. The core catalyst for this reaction has been proved to be the palladium-based catalyst[18-19]. But the price of Pd is so expensive that the development of this reaction in industry has been greatly restricted[20]; and reducing the amount of Pd in this reaction has become a hot topic in academia[21-22]. This problem can be well solved by making metal Pd into single-atom catalysts. Besides, Pd SACs also show excellent performance in a large number of catalytic reac-

* Foundation item: Project (21736007) supported by the Key Projects of National Science Foundation of China, project (21576178, 21476155) supported by the National Science Foundation of China, project (2016-030) supported by Shanxi Scholarship Council of China and project (J18-19-602) supported by the Foundation of State Key Laboratory of Coal Conversion.
1) College of Chemistry and Chemical Engineering, Taiyuan University of Technology, 030024 Taiyuan, China; 2) Key Laboratory of Coal Science and Technology of Ministry of Education and Shanxi Province, Taiyuan University of Technology, 030024 Taiyuan, China; 3) State Key Laboratory of Coal Conversion, Institute of Coal Chemistry, Chinese Academy of Sciences, 030001 Taiyuan, China
Author: LIN Hao, E-mail: 13303067126@163.com
Recieved date: 2018-12-17; Revised date: 2019-02-18

tions[23-24]. In the study of PEI et al[25], Pd SACs were applied in selective hydrogenation of acetylene, the results show that Pd SACs have an excellent activity and selectivity for the reaction, and the utilization ratio of precious metal Pd has been greatly improved by Pd SACs.

The interactions between two kinds of metals make bimetallic catalysts show a unique electronic structure and chemical properties[26-27]. The key step in the preparation of alloy catalysts is the selection of second metal. In our past research studies, Pd-Al and Pd-Cu bimetallic catalysts had been widely used in a large number of chemical reactions due to their excellent properties[28]. For example, Pd-Al bimetallic catalysts show a good catalytic performance for the generation of DMO in our previous work[29-30]. And PARK et al[31] synthesized CeO_2-supported Pd-Cu alloy catalyst with one-pot method for the oxidation of formic acid, the experimental results show that the catalytic performance of this catalyst is much better than those of other catalysts.

As mentioned above, Pd-Al and Pd-Cu bimetallic catalysts all have played important roles in the field of catalytic, however, the effect of Pd_1-M (M=Al, Cu) single-atom catalysts on the reaction mechanism of CO oxidative coupling to DMO is not clear. In our previous studies, we have found that the surface structure of Pd(100) had a high activity in CO oxidative coupling to DMO, but the selectivity of Pd(100) surface to generate DMO needed to be improved. So in this work, the models of Pd_1-M (M=Al, Cu) bimetallic single－atom catalysts with (100) surface properties have been constructed. And based on theoretical calculation, the reaction process of CO oxidative coupling to DMO on these catalysts has been clarified. It is expected that this work can provide a new idea for preparing catalysts for synthesis of DMO with superior performance and low Pd consumption in industry.

1　Method and models

1.1　Computational methods and parameters

All data in this work were calculated by using Vienna Ab-initio Simulation Package (VASP) software[32-34]. The core-valence interaction was described by the projector-augmented wave (PAW) method. And the generalized gradient approximation (GGA) with the Perdew-Burke-Ernzerhof (PBE)[35] exchange-correlation functional was used in this work. The plane wave basis set with cutoff energy of 400 eV was used. The k-point was selected as $3\times2\times1$ for Pd_1-Al and Pd_1-Cu SACs. The atomic structures were relaxed until the electronic energy was less than 1×10^{-5} eV and force was less than 0.3 eV/nm for unconstrained atoms. The Climbing-image Nudged Elastic Band method (CI-NEB)[36-37] combining with the dimer method[38-39] was used for locating transition state (TS) for every elementary step, in which the force was converged to 0.5 eV/nm. Vibrational frequency calculation was done and only one virtual frequency was obtained to confirm the TS structure.

The activation energy (E_a) can be obtained by the following Equation:

$$E_a = E_{TS} - E_R \tag{1}$$

And the adsorption energy (E_{ads}) is defined as the following formula:

$$E_{ads} = E_{slab} + E_{adsorbate} - E_{slab/ladsorbate} \tag{2}$$

Where E_{slab} and $E_{adsorbate}$ represent the energies of different surfaces and the isolated adsorbate in the gas phase, respectively. $E_{slab/adsorbate}$ is the total energy of an adsorption system.

1.2　Construction of models

First of all, the pure Al(100) and Cu(100) surfaces are modeled using a $p(3\times4)$ unit cell with three layers. The optimized lattice parameters of Al and Cu are 0.399 2 nm and 0.362 3 nm, respectively. Which is in line with the experimental dates (Al, 0.404 9 nm; Cu, 0.361 5 nm)[40]. Next, an atom in the top layer of pure Al(100) and Cu(100) surfaces will be replaced by a Pd atom. Finally, through structural optimization we will get Pd_1-Al and Pd_1-Cu SACs.

For Pd_1-Al and Pd_1-Cu SACs, the third layer was frozen in the bulk position, other layers and adsorbed species were allowed to relax. All species

on these surfaces were allowed to relax. The structures and adsorption sites on Pd_1-Al and Pd_1-Cu SACs are shown in Fig.1. Considering the location of the active center, there are only three possible active sites on Pd_1-Al and Pd_1-Cu SACs (bridge, top-Pd and hollow) being studied for DMO formation.

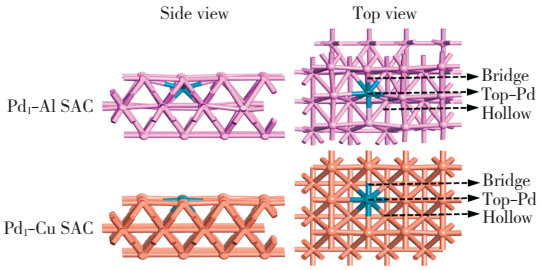

Fig.1 Structures of Pd_1-Al and Pd_1-Cu SACs and corresponding adsorption sites

2 Results and discussion

2.1 Pathway to generate DMO

For the reaction process of CO oxidative coupling to DMO, some conclusions can be obtained by referring to our early work and previous studies: the dissociation of CH_3ONO is favorable[41-42], and the product OCH_3 will directly initiate the oxidative coupling reaction; there are mainly two ways to generate DMO[43], as shown in Fig.2, including $COOCH_3$ coupling with $COOCH_3$ (Path 1) and $COOCH_3$ coupling with CO (Path 2). The by-product dimethyl-carbonate (DMC) comes from Path 1. Through studying the formation of DMC, the selectivity of catalysts to the target product will be clarified.

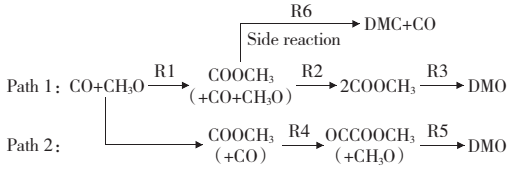

Fig.2 Pathways of CO oxidative coupling to DMO

2.2 Adsorption properties of reactants, possible intermediates and products

First of all, the optimized structure of Pd_1-Al SAC is very unstable as shown in Fig.1. This is mainly due to the relatively softer physical structural property of Al. We have further studied the adsorbability of Pd_1-Al SAC to reactive species, the results show that after adsorbing reaction species the surface structure of Pd_1-Al SAC is greatly deformed, and cannot continue to participate in the reaction. So we can conclude that Al is not a suitable metal to act as the substrate of a single-Pd-atom catalyst. In this study, a disadvantage of SACs is that the structural deformation during the reaction process is obviously comparable with that of other types of bimetallic catalysts[29-30]. Thus it can be seen that there are still some challenges in the comprehensive application of SACs in the field of catalysis.

The adsorption configurations and corresponding adsorption energies of related species on Pd_1-Cu SAC are shown in Fig.3.

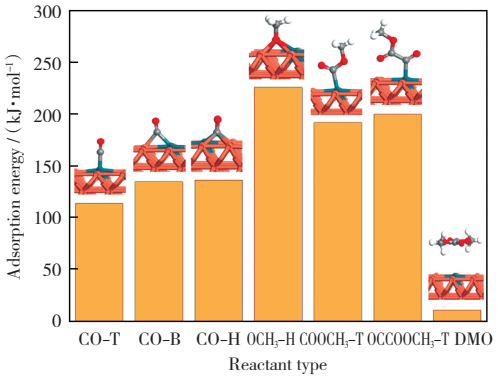

Fig.3 Adsorption configurations of reactive species on Pd_1-Cu SAC and corresponding adsorption energies

CO has three adsorption modes on Pd_1-Cu SAC, they are adsorbed at the top, bridge and hollow sites of the catalyst surface by C atom. And the corresponding adsorption energies of CO on Pd_1-Cu SAC are 113.9 kJ/mol, 134.9 kJ/mol, and 136.4 kJ/mol, respectively. Unlike CO, OCH_3 can only be adsorbed stably on the hollow site with the adsorption energy of 226.1 kJ/mol. The adsorption mode of $COOCH_3$ on Pd_1-Cu SAC is the top adsorption on the Pd atom. The adsorption energy of $COOCH_3$ Pd_1-Cu SAC is 192.1 kJ/mol. And the adsorption mode of $OCCOOCH_3$ on Pd_1-Cu SAC

binds with Pd atom on surface through C atom with the adsorption energy of 200.1 kJ/mol.

DMO exists on Pd_1-Cu SAC in the form of physical adsorption which is in good agreement with our previous studies[15,29-30]. And the adsorption energy of DMO on Pd_1-Cu SAC is only 10.6 kJ/mol. It is worth mentioning that the OCCO which acts as an important intermediate on pure Pd (111) surface[29] cannot exist stably on Pd_1-Cu SAC.

2.3　CO oxidative coupling to DMO on Pd_1-Cu SAC

The generation of DMO on Pd_1-Cu SAC begins with the formation of co-adsorption configuration of CO and OCH_3. At this time, CO and OCH_3 are adsorbed at the bridge site formed by Pd and Cu atoms. Then CO reacts with OCH_3 to form $COOCH_3$. This process requires a transition state (TS1) and overcomes an energy barrier of 55.3 kJ/mol with an endotherm of 20.1 kJ/mol. In this step, the distance between C of CO and O of OCH_3 has been shortened from 0.365 2 nm to 0.133 7 nm in $COOCH_3$. After the generation of $COOCH_3$, the next reaction will be divided into two paths down (Path 1 and Path 2).

In Path 1, the $COOCH_3$ will be formed via a transition state (TS2), as shown in Fig.4. Activation energy of 25.6 kJ/mol is needed to complete this process with an exothermic heat of 27.8 kJ/mol. The distance between C of CO and O of OCH_3 has been shortened from 0.340 1 nm to 0.135 1 nm. The generation of DMO is accomplished by the coupling of two $COOCH_3$. This process has to overcome an energy barrier of 97.9 kJ/mol and releases exothermic heat of 12.7 kJ/mol, meanwhile the distance between two C atoms changes from 0.296 3 nm to 0.198 1 nm in TS3 and eventually becomes 0.154 7 nm in DMO.

In Path 2, the formed $COOCH_3$ will be coupled with a CO to produce $OCCOOCH_3$ at the beginning. This process needs to go through a transition state (TS4) by overcoming an energy barrier of 152.0 kJ/mol and endothermic heat of 43.0 kJ/mol. The distance between those two carbon atoms is reduced from 0.307 6 nm to 0.155 6 nm. In the final phase of Path 2, the $OCCOOCH_3$ reacts with another OCH_3 to form DMO. The energy barrier of this elementary reaction is 90.6 kJ/mol and exothermic heat is 25.7 kJ/mol.

It is not difficult to find that Path 1 is the favorable route for the formation of DMO on Pd_1-Cu SAC. The rate-determining step of each path is the coupling reaction of two C atoms in both paths of generating DMO. That is, the coupling reaction of two $COOCH_3$ and Path 1 and in Path 2 is the coupling reaction of $COOCH_3$ and CO. This is in good agreement with our previous research[29].

When $COOCH_3$, CO and OCH_3 are adsorbed on the Pd_1-Cu SAC at the same time, OCH_3 does not react with CO to form a second $COOCH_3$, but react with the formed $COOCH_3$ to produce the DMC, as shown in Fig.4. Similarly, this process also needs to undergo a transition state (TS6). The energy barrier of this reaction is 82.8 kJ/mol, simultaneous exothermic heat is 115.3 kJ/mol. The distance between O of OCH_3 and C of $COOCH_3$ is reduced from 0.289 9 nm to 0.134 3 nm.

2.4　Micro-kinetic modeling

The micro-kinetic modeling is an effective way to analyze the performance of catalysts. Its reliability has been confirmed by numerous studies in the past[44-48]. In our previous work, the formation rate of DMO on Pd(111), Pd-Cu(111) and Pd-Al(111) surfaces has been well investigated by micro-kinetic modeling. In order to further understand the effects of Pd_1-Cu SAC toward CO oxidative coupling to DMO, we have also carried out the calculation of corresponding kinetic and Turnover Frequency (TOF). At the same time, the selectivity of catalyst to DMO will be further clarified by kinetic model. First of all, the elementary reactions involved in the whole reaction process are listed in Table 1.

The rate constants of all elementary reactions as shown in Table 1 are calculated by the harmonic transition state theory (TST), and the formula (3) for calculation is as follows[49-50]:

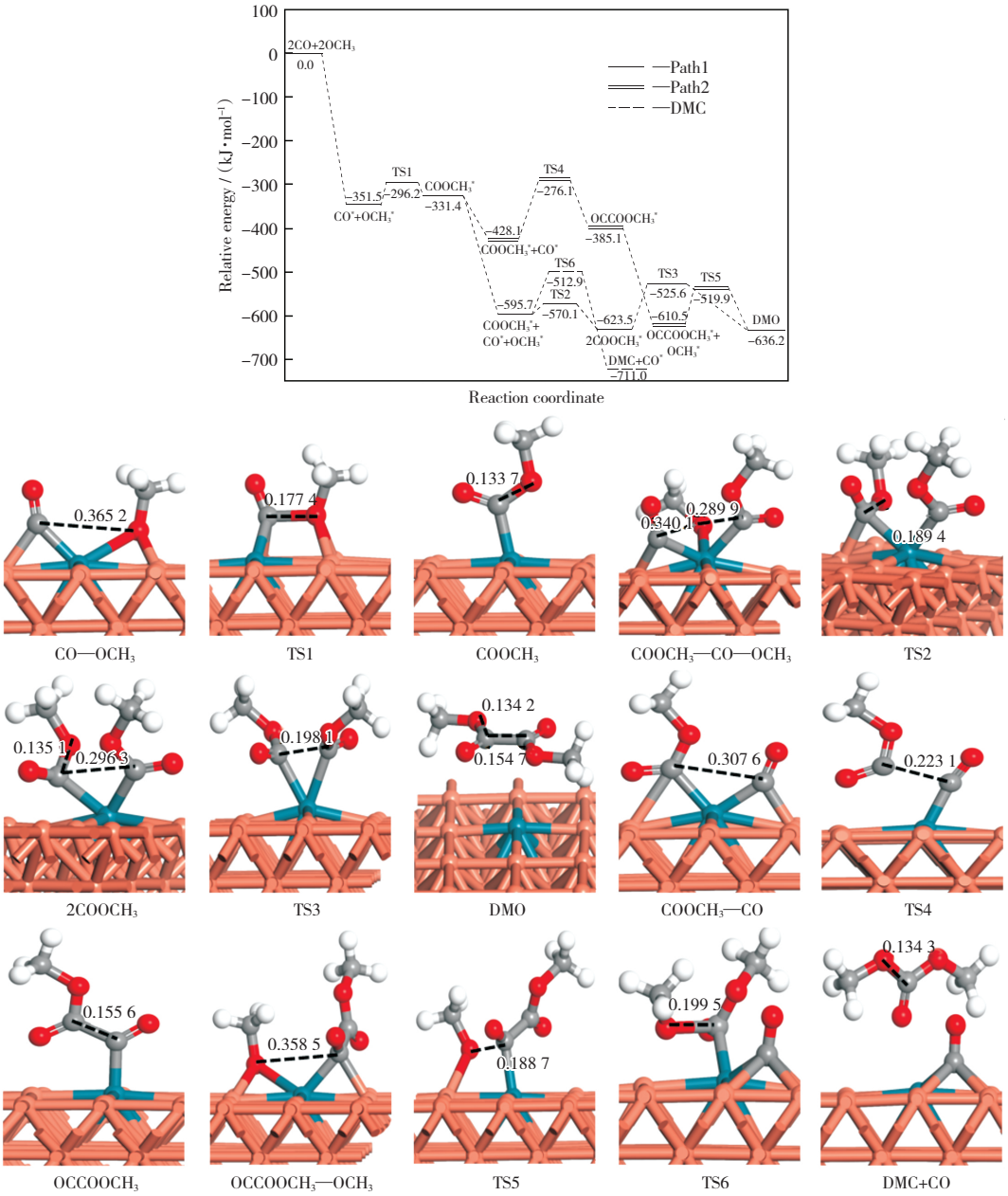

Fig.4 Relative energy diagram of DMO formation and the configuration of the species involved in the reaction on the Pd_1-CuSAC(energy unit:nm)

Table 1 Related reactions and the corresponding rate constants

Reaction	Rate constant
$CO^* + OCH_3^* \longrightarrow COOCH_3^* + *$	k_1
$COOCH_3^* + CO^* + OCH_3^* \longrightarrow 2COOCH_3^* + *$	k_2
$2COOCH_3^* \longrightarrow DMO + 2*$	k_3
$COOCH_3^* + CO^* \longrightarrow OCCOOCH_3^* + *$	k_4
$OCCOOCH_3^* + OCH_3^* \longrightarrow DMO + 2*$	k_5
$COOCH_3^* + CO^* + OCH_3^* \longrightarrow DMC + CO^* + 2*$	k_6

$$k_i = v_i \exp\left(\frac{-E_a}{RT}\right) \tag{3}$$

And the surface coverage of CO, OCH_3 and intermediates (θ_{CO}, θ_{OCH_3}, θ_{COOCH_3}, and $\theta_{OCCOOCH_3}$) can be obtained from the steady-state approximation theory[51]. At the same time, the equilibrium relationship between reactive species and free site (θ^*) can also be obtained. The formulas used in the calculation are as follows (4)-(8):

$$\theta_{OCH_3} = P_{OCH_3} K_{OCH_3} \theta^* \tag{4}$$

$$\theta_{CO} = P_{CO} K_{CO} \theta^* \tag{5}$$

$$\theta_{COOCH_3}: \frac{d\theta_{COOCH_3}}{dt} = k_1 \theta_{OCH_3} \theta_{CO} + k_2 \theta_{OCH_3} \theta_{CO} - k_3 \theta_{COOCH_3}^2 - k_4 \theta_{COOCH_3} \theta_{CO} - k_6 \theta_{COOCH_3} \theta_{OCH_3} = 0 \tag{6}$$

$$\theta_{OCCOOCH_3}: \frac{d\theta_{OCCOOCH_3}}{dt} = k_4 \theta_{COOCH_3} \theta_{CO} -$$

$$k_5\theta_{OCCOOCH_3}\theta_{OCH_3}=0 \quad (7)$$

$$\theta_{CO}+\theta_{OCH_3}+\theta_{COOCH_3}+\theta_{OCCOOCH_3}+\theta^*=1 \quad (8)$$

Previous experimental studies have shown that the suitable temperature range for the reaction is 375 K-415 K, and the partial pressures of CO and OCH_3 are 280 kPa and 200 kPa[52], respectively. The relevant computational data are listed in Table 2.

Table 2　Reaction equilibrium constants, rate constants and the free site (θ^*) in the reaction on the Pd_1-Cu SAC (375 K≤T≤415 K)

Temperature/K	$K_{CO}/10^{15}$	$K_{OCH_3}/10^{32}$	$k_1/10^4$	$k_2/10^9$	$k_3/10^{-4}$	$k_4/10^{-8}$	$k_5/10^2$	$k_6/10^0$	$\theta^*/10^{-41}$
375	1.43	2.83	5.99	2.78	3.79	4.89	3.07	2.06	4.65
385	0.462	0.429	9.54	3.50	8.70	17.70	6.63	4.16	25.30
395	0.158	0.071 4	14.80	4.36	19.10	60.20	13.70	8.09	126
405	0.057 1	0.013 0	22.50	5.36	40.60	19.30	27.50	15.20	583
415	0.021 6	0.002 56	33.50	6.53	82.30	58.30	53.30	27.80	2 500

The meaning of turnover frequency (TOF) is a conversion amount of products at a single active site in unit time[53-55]. And this concept focuses on the description of the active sites of catalysts. Because of the special structure of SACs, the formation rate of products is equal to the TOF value of products. It is generally known that the formation rate of DMO and DMC is directly proportional to the concentration of reactants and the rate constants[56]. And the formation rate of DMO and DMC can be obtained via the following formula (9)-(10):

$$r_{DMO}=k_3\theta^2_{COOCH_3}+k_5\theta_{OCCOOCH_3}\theta_{OCH_3} \quad (9)$$

$$r_{DMC}=k_6\theta_{COOCH_3}\theta_{OCH_3} \quad (10)$$

The TOF values of DMO and DMC on Pd_1-Cu SACs are listed in Table 3. Comparing this study with our previous work, it can be found that the formation rate of DMO on Pd_1-Cu SAC is much higher than that on pure Pd surface[29]. And the formation rate of DMO increases with the increase of temperature, so it can be concluded that increasing temperature is beneficial to the formation of DMO.

Table 3　TOF (s^{-1}) of DMO and DMC on the Pd_1-Cu SAC (375 K≤T≤415 K)

Temperature/K	TOF/s^{-1}	
	DMO	DMC
375	3.77×10^{-4}	5.42×10^{-3}
385	8.67×10^{-4}	9.00×10^{-3}
395	1.91×10^{-3}	1.46×10^{-2}
405	4.04×10^{-3}	2.30×10^{-2}
415	8.26×10^{-3}	3.55×10^{-2}

In order to further describe the catalytic performance of catalyst to CO oxidative coupling to DMO, we plot a temperature-dependent curve of the selectivity of catalyst to DMO. As shown in Fig.5, it is not difficult to find that the selectivity of Pd_1-Cu SAC to DMO formation is not ideal. At 375 K, the selectivity of Pd_1-Cu SAC to DMO formation is only 6.5%. Even when the temperature rises to 415 K, the selectivity is still relatively low (only 18.8%). And the selectivity of Pd_1-Cu SAC to DMO also increases with the increase of temperature; therefore, we can promote the selectivity of catalyst to the formation of DMO by increasing temperature.

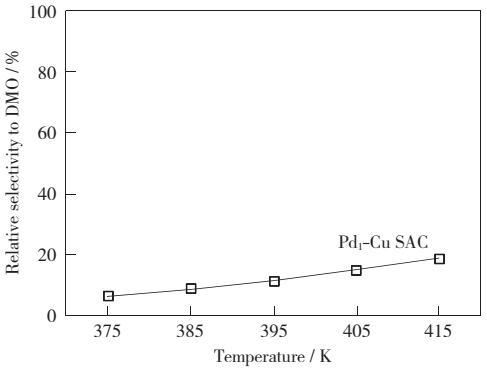

Fig.5　Relative selectivity of DMO formation on the Pd_1-Cu SAC

3　Conclusions

In this study, we have constructed Pd_1-M (M=Al, Cu) single-atom catalysts (SACs). And the reaction mechanism of CO oxidative coupling to DMO over these catalysts has been simulated by DFT calculation. Through the analysis of the calculation results, we can get the following conclusions. Firstly, the structural of Pd_1-Al SAC is instable, so it cannot further catalyze the oxidative coupling reaction of CO to achieve the purpose of

preparing DMO. Secondly, Pd_1-Cu SAC has a high activity for the generation of DMO, and DMO mostly comes from the coupling of two $COOCH_3$. Last but not least, the application of Pd_1-Cu SAC has greatly reduced the amount of precious metal Pd. However, Pd_1-Cu SAC is more conducive to the generation of DMC, and the selectivity of Pd_1-Cu SAC to DMO is not ideal. In the future, we will conduct further in-depth studies on this issue in order to obtain better catalysts.

References

[1] QIAO Botao, WANG Aiqin, Yang Xiaofeng, *et al*. Single-atom Catalysis of CO Oxidation Using Pt_1/FeO_x [J]. Nat Chem, 2011, 3(8): 634-641.

[2] THOMAS J M, SAGHI Z, GAI P L. Can a Single Atom Serve as the Active Site in Some Heterogeneous Catalysts? [J]. Top Catal, 2011, 54(10-12): 588-594.

[3] MICAELA C Q, ARTUR Y, JIN Mingshang, *et al*. Structure Sensitivity of Alkynol Hydrogenation on Shape- and Size-controlled Palladium Nanocrystals: Which Sites Are Most Active and Selective? [J]. J Am Chem Soc, 2011, 133(32): 12787-12794.

[4] LOPEZ N, JANSSENS T V W, CLAUSEN B S, *et al*. On the Origin of the Catalytic Activity of Gold Nanoparticles for Low-temperature CO Oxidation[J]. J Catal, 2004, 223(1): 232-235.

[5] SUN Shuhui, ZHANG Gaixia, GAUQUELIN Nicolas, *et al*. Single-atom Catalysis Using Pt/Graphene Achieved Through Atomic Layer Deposition[J]. Scientific Reports, 2013, 3: 1755-1763.

[6] WU Ping, DU Pan, ZHANG Hui, *et al*. Graphyne-supported Single Fe Atom Catalysts for CO Oxidation[J]. Phys Chem Chem Phys, 2015, 17(2): 1441-1449.

[7] HE Bingling, SHEN Jiansheng, TIAN Zhixue. Iron-embedded C_2N Monolayer: a Promising Low-cost and High-activity Single-atom Catalyst for CO Oxidation[J]. Phys Chem Chem Phys, 2016, 18(35): 24261-24269.

[8] ZHANG Haijun, WATANABE T, OKUMURA M, *et al*. Catalytically Highly Active Top Gold Atom on Palladium Nanocluster[J]. Nature Materials, 2012, 11(1): 49-52.

[9] KYRIAKOU G, BOUCHER M B, JEWELL A D, *et al*. Isolated Metal Atom Geometries as a Strategy for Selective Heterogeneous Hydrogenations[J]. Science, 2012, 335(6073): 1209-1212.

[10] LI Xiaogang, BI Wentuan, ZHANG Lei, *et al*. Single-atom Pt as Co-catalyst for Enhanced Photocatalytic H_2 Evolution[J]. Advanced Materials, 2016, 28(12): 2427-2431.

[11] LIN Jian, WANG Aiqin, QIAO Botao, *et al*. Remarkable Performance of Ir_1/FeO_x Single-atom Catalyst in Water Gas Shift Reaction[J]. J Am Chem Soc, 2013, 135(41): 15314-15317.

[12] LONG Bo, TANG Yan, LI Jun. New Mechanistic Pathways for CO Oxidation Catalyzed by Single-atom Catalysts: Supported and Doped Au_1/ThO_2[J]. Nano Research, 2016, 9(12): 3868-3880.

[13] DING K, GULEC A, JOHNSON A M, *et al*. Identification of Active Sites in CO Oxidation and Water-gas Shift over Supported Pt Catalysts[J]. Science, 2015, 350(6257): 189-192.

[14] ZHAO Xiuge, LIN Qian, XIAO Wende. Characterization of Pd-CeO_2/α-alumina Catalyst for Synthesis of Dimethyl Oxalate [J]. Appl Catal A, 2005, 284(1): 253-257.

[15] HAN Bingying, LIN Hao, LING Lixia, *et al*. A DFT Study on Dimethyl Oxalate Synthesis over PdML/Ni(111) and PdML/Co(111) Surfaces[J]. Appl Surf Sci, 2018, 465: 498-508.

[16] ZHAO Yujun, ZHANG Yaqing, WANG Yue, *et al*. Structure Evolution of Mesoporous Silica Supported Copper Catalyst for Dimethyl Oxalate Hydrogenation[J]. Appl Catal A: General, 2017, 539: 59-69.

[17] ZHAO Li, ZHAO Yujun, WANG Shengping, *et al*. Hydrogenation of Dimethyl Oxalate Using Extruded Cu/SiO_2 Catalysts: Mechanical Strength and Catalytic Performance[J]. Ind Eng Chem Res, 2012, 51(43): 13935-13943.

[18] YAMAMOTO Y. Vapor Phase Carbonylation Reactions Using Methyl Nitrite over Pd Catalysts[J]. Catal Surv Asia, 2010, 14(3/4): 103-110.

[19] UCHIUMI S I, ATAKA K, MATSUZAKI T. Oxidative Reactions by a Palladium-alkyl Nitrite System[J]. J Organomet Chem, 1999, 576(1): 279-289.

[20] PENG Siyan, XU Zhongning, CHEN Qingsong, *et al*. MgO: an Excellent Catalyst Support for CO Oxidative Coupling to Dimethyl Oxalate[J]. Catal Sci Technol, 2014, 4(7): 1925-1930.

[21] WANG Zhiqiao, XU Zhongning, PENG Siyan, *et al*. New Catalysts for Coal to Ethylene Glycol[J]. Chin J Chem, 2017, 35(6): 759-768.

[22] JIANG Xuanzhen, SU Yuehua, LEE B J, *et al*. A Study on the Synthesis of Diethyl Oxalate over Pd/α-Al_2O_3 Catalysts[J]. Appl Catal A, 2001, 211(1): 47-51.

[23] CAO Xinrui, JI Yongfei, LUO Yi. Dehydrogenation of Propane to Propylene by a Pd/Cu Single-atom Catalyst: Insight from First-principles Calculations[J]. J Phys Chem C, 2015, 119(2): 1016-1023.

[24] VILE G, ALBANI D, NACHTEGAAL M, *et al*. Ein Stabiler "Single-site"-palladiumkatalysator Für Hydrierungen[J]. Angew Chem Int Ed, 2015, 127: 11417-11422.

[25] PEI Guangxian, LIU Xiaoyan, CHAI Mengqian, *et al*. Isolation of Pd Atoms by Cu for Semi-hydrogenation of Acetylene: Effects of Cu Loading[J]. Chinese J Catal, 2017, 38(9): 1540-1548.

[26] KITCHIN J R, NØRSKOV J K, BARTEAU M A, *et al*. Role of Strain and Ligand Effects in the Modification of the Electronic and Chemical Properties of Bimetallic Surfaces[J]. Phys Rev Lett, 2004, 93(15): 156801.

[27] STRASSER P, KOH S, ANNIYEV T, *et al*. Lattice-strain Control of the Activity in Dealloyed Core-shell Fuel Cell Catalysts [J]. Nat Chem, 2010, 2(6): 454-460.

[28] LI Shaojie, CHENG Daojian, QIU Xiangguo, *et al*. Synthesis of Cu@Pd Core-shell Nanowires with Enhanced Activity and Stability for Formic Acid Oxidation[J]. Electrochim Acta, 2014, 143(10): 44-48.

[29] HAN Bingying, FENG Xue, LING Lixia, *et al*. CO Oxidative Coupling to Dimethyl Oxalate over Pd-Me (Me=Cu, Al) Catalysts: a Combined DFT and Kinetic Study[J]. Phys Chem Chem Phys, 2018, 20(10): 7317-7332.

[30] FENG Xue, LING Lixia, CAO Yueting, *et al*. A DFT Study on the Catalytic CO Oxidative Coupling to Dimethyl Oxalate on Al-doped Core-shell Pd Clusters[J]. J Phys Chem C, 2017, 122(2): 1169-1179.

[31] PARK K H, LEE Y W, KIM Y, *et al*. One-pot Synthesis of CeO_2-supported Pd-Cu-alloy Nanocubes with High Catalytic Activity[J]. Chem Eur J, 2013, 19: 8053-8057.

[32] KRESSE G, HAFNER J. Ab Initio Molecular Dynamics for Open-shell Transition Metals[J]. Phys Rev B, 1993, 48(17): 13115-13118.

[33] KRESSE G, FURTHMÜLLER J. Efficient Iterative Schemes for Ab Initio Total-energy Calculations Using a Plane-wave Basis Set[J]. Phys Rev B, 1996, 54(16): 11169-11186.

[34] KRESSE G, JOUBERT D. From Ultrasoft Pseudopotentials to the Projector Augmented-wave Method[J]. Phys Rev B, 1999, 59(3): 1758-1775.

[35] PERDEW J P, BURKE K, ERNZERHOF M. Generalized Gradient Approximation Made Simple[J]. Phys Rev Lett, 1996, 77 (18): 3865-3868.

[36] SHEPPARD D, XIAO Penghao, CHEMELEWSKI W, *et al*. A Generalized Solid-state Nudged Elastic Band Method[J]. J Chem Phys, 2012, 136: 074103.

[37] SHEPPARD D, TERRELL R, HENKELMAN G. Optimization Methods for Finding Minimum Energy Paths[J]. J Chem Phys, 2008, 128(13): 134106.

[38] HENKELMAN G, JÓNSSON H. A Dimer Method for Finding Saddle Points on High Dimensional Potential Surfaces Using Only First Derivatives[J]. J Chem Phys, 1999, 111(15): 7010-7022.

[39] OLSEN R A, KROES G J, HENKELMAN G, *et al*. Comparison of Methods for Finding Saddle Points Without Knowledge of the Final States[J]. J Chem Phys, 2004, 121(20): 9776-9792.

[40] ASHCROFT N W, MERMIN N D. Solid State Physics[M]. Rochester: Saunders College Publishing, 1976.

[41] CASSADY C J, FREISER B S. Gas-phase Reactions of Transition-metal Ions with Methyl Nitrite and Nitromethane[J]. J Am Chem Soc, 1985, 107(6): 1566-1573.

[42] FAN Chen, LUO Man, XIAO Wende. Reaction Mechanism of Methyl Nitrite Dissociation During CO Catalytic Coupling to Dimethyl Oxalate: a Density Functional Theory Study[J]. Chinese J Chem Eng, 2016, 24(1): 132-139.

[43] LI Qiaohong, ZHOU Zhangfeng, CHEN Ruiping, *et al*. Insights into Reaction Mechanism of CO Oxidative Coupling to Dimethyl Oxalate over Palladium: a Combined DFT and IR Study[J]. Phys Chem Chem Phys, 2015, 17(44): 9126-9134.

[44] LIU Ping, LOGADOTTIR A, NØRSKOV J K. Modeling the Electro-oxidation of CO and H_2/CO on Pt, Ru, PtRu and Pt_3Sn [J]. Electrochim Acta, 2003, 48(25): 3731-3742.

[45] LIU Ping, RODRIGUEZ J A. Water-gas-shift Reaction on Molybdenum Carbide Surfaces: Essential Role of the Oxycarbide [J]. J Phys Chem B, 2006, 110(39): 19418-19425.

[46] OVESEN C V, STOLTZE P, NØRSKOV J K, *et al*. A Kinetic Model of the Water Gas Shift Reaction[J]. J Catal, 1992, 134 (2): 445-468.

[47] CHOI Y M, LIU Ping. Mechanism of Ethanol Synthesis from Syngas on Rh(111)[J]. J Am Chem Soc, 2009, 131(36): 13054-13061.

[48] ZUO Zhijun, PENG Fen, HUANG Wei. Efficient Synthesis of Ethanol from CH_4 and Syngas on a Cu-Co/TiO_2 Catalyst

Using a Stepwise Reactor[J].Sci Rep,2016,6:34670.
[49] HUANG Liangfeng,NI Meiyan,ZHANG Guoren,*et al*.Modulation of the Thermodynamic,Kinetic,and Magnetic Properties of the Hydrogen Monomer on Graphene by Charge Doping[J].J Phys Chem C,2011,135(6):(Article 064705)1-9.
[50] HUANG Liangfeng,NI Meiyan,ZHENG Xiaohong,*et al*.Ab Initio Simulations of the Kinetic Properties of the Hydrogen Monomer on Graphene[J].J Phys Chem C,2010,114(51):22636-22643.
[51] BLAKEMORE J E,CORCORAN W H.Validity of the Steady-state Approximation Applied to the Pyrolysis of N-butane[J].Ind Eng Chem Process Des Dev,1969,8(2):206-209.
[52] XU Zhongning,SUN Jing,LIN Chensheng,*et al*.High-performance and Long-lived Pd Nanocatalyst Directed by Shape Effect for CO Oxidative Coupling to Dimethyl Oxalate[J].ACS Catal,2012,3(2):118-122.
[53] BOUDART M,ALDAG A,BENSON J E,*et al*.On the Specific Activity of Platinum Catalysts[J].J Catal,1966,6(1):92-99.
[54] BOUDART M.Turnover Rates in Heterogeneous Catalysis[J].Chem Rev,1995,95(3):661-666.
[55] BOUDART M.Catalysis by Supported Metals[J].Adv Catal,1969,20:153-166.
[56] FU Xiancai,SHEN Wenxia,YAO Tianyang,*et al*.Physical Chemistry[M].5th Edition.Beijing:Higher Education Press:2009.

Pd_1-M(M=Al,Cu)单原子催化剂上 CO 氧化偶联制 DMO 的理论研究

林 浩[1)] 韩冰莹[2)] 凌丽霞[1,3)] 刘 平[3)] 章日光[2)] 王宝俊[2)]
(1.太原理工大学化学化工学院,030024 太原;2.太原理工大学煤科学与技术教育部重点实验室,030024 太原;3.煤转化国家重点实验室,中国科学院山西煤炭化学研究所,030001 太原)

摘 要 为了减少 CO 氧化偶联制 DMO 反应中 Pd 催化剂的用量,设计了一系列单原子 Pd 催化剂,并通过 DFT 理论计算详细研究了 Pd_1-M(M=Al,Cu)单原子催化剂(SACs)对该反应的影响。结果表明:首先,由于 Pd_1-Al SAC 结构不稳定,导致该催化剂不能用于 CO 氧化偶联制 DMO 反应;其次,Pd_1-Cu SAC 对该反应有出色的活性,同时也达到了减少贵金属 Pd 用量的目的,但其对 DMO 生成的选择性很不理想,需要在后续的研究中进一步提高。

关键词 CO 氧化偶联制 DMO,单原子催化,Pd 基催化剂,密度泛函理论
中图分类号 TQ426

(责任编辑 刘改换)